Available online at www.sciencedirect.com
ScienceDirect
Journal of Photochemistry and Photobiology A: Chemistry 187 (2007) 64–71
Journal of Photochemistry and Photobiology A:Chemistry
www.elsevier.com/locate/jphotochem

Synthesis and photoinduced intramolecular charge transfer of *N*-substituted 1,8-naphthalimide derivatives in homogeneous solvents and in presence of reduced glutathione

Sujan Chatterjee [a], Smritimoy Pramanik [a], Sk Ugir Hossain [b], Sudin Bhattacharya [b,*], Subhash Chandra Bhattacharya [a,*]

[a] *Department of Chemistry, Jadavpur University, Kolkata 700032, India*
[b] *Department of Cancer Chemoprevention, Cittaranjan National Cancer Research Institute, Kolkata 700026, India*

Received 7 May 2006; received in revised form 5 August 2006; accepted 26 September 2006
Available online 7 October 2006

Abstract

Ground and excited state properties of newly synthesized *N*-substituted naphthalimide derivatives (**3a–c**) have been investigated in protic and aprotic solvents of varying polarity. These studies focused identification of the π, π* and charge transfer to solvent (CTTS) transitions. Excited state properties have been rationalized in terms of photoinduced intramolecular charge transfer (PICT) process. Effect of protic solvent and aprotic solvent on the PICT process has also been determined. Excited state PICT process of the compounds has also been studied in aqueous solution of H-bonding agent reduced L-glutathione (GSH).

Keywords: Naphthalimide; CTTS; Fluorophores; PICT; Reduced glutathione

1. Introduction

1,8-Naphthalimides are generally fluorescent compounds for which a series of biological (local anaesthetics [1], DNA-cleaving agents [2], tumoricidals [3] and non-biological (optical brighteners [4], lucifer dyes [5]) applications have been found. 1,8-Naphthalimide and bisnaphthalimide derivatives are promising anticancer agents [6,7], the sulfonated derivatives are good antiviral agents with selective in vitro activity against the human immunity deficiency virus, HIV-1 [8]. Brominated mono and bisnaphthalimide derivatives are photochemotherapeutic inhibitors for enveloped viruses in blood and blood products [9–11]. The photoactivity and DNA-intercalation properties of 1,8-naphthalimide derivatives have also prompted studies on sequence-specific DNA-photonucleases [12].

Kossanyi and co-workers [13–15] extensively studied the spectroscopic and photophysical properties of various naphthalimide derivatives. In some of these studies, influence of the geometry of the molecule or intramolecular geometrical relaxation process on the emitting properties of the molecules has been investigated. Brown and co-workers [16,17] studied the photophysical properties of aminonaphthalimides in various media. While the fluorescence quantum yield of 4-aminonaphthalimide was as high as 0.8 in some media, nonradiative transition was found to be quite efficient in aqueous solution [18]. The enhanced nonradiative rate in aqueous media was attributed to the formation of a hydrogen-bonded cluster between the probe and solvent molecules. This group also studied the effect of pH of the medium on the fluorescence properties of aminonaphthalimides.

Samanta et al. [19,20] studied transition metal ion induced fluorescence sensing in newly synthesized amino and substituted amino-naphthalimide derivatives. Recently they studied conformation dependent intramolecular charge transfer behavior of 4-amino-1,8-naphthalimide derivatives differing in the amino functionality as a function of the polarity of the medium [21]. Martin et al. [22] studied inhibition of intramolecular charge transfer process of 4-methoxy and 4-acetamide *N*-substituted 1,8-naphthalimide derivatives in protic solvents

* Corresponding authors. Tel.: +91 33 2414 6223; fax: +91 33 2414 6584.
E-mail addresses: sudinb19572004@yahoo.co.in (S. Bhattacharya), sbjuchem@yahoo.com (S.C. Bhattacharya).

1010-6030/$ – see front matter © 2006 Elsevier B.V. All rights reserved.
doi:10.1016/j.jphotochem.2006.09.013

having H-bonding ability and by addition of protons from acid and solvents.

In the present study, photophysical properties of some newly synthesized 1,8-naphthalimide derivatives (**3a**, **3b** and **3c**) have been observed in solvents of varying polarity as well as having different H-bonding ability. In 1,8-naphthalimide derivatives PICT process occurs and PICT becomes more favorable in polar protic solvents ethanol compared to the polar aprotic solvent acetonitrile. Reduced glutathione having H-bonding ability [23], can inhibit PICT process of **3a** and **3b** whereas it exerts no effect on the PICT process of **3c**. Substituent dependent variation of PICT process has also been illustrated in the present observation.

2. Experimental

2.1. Materials

1,8-Naphthalic anhydride, the starting materials for the synthesis of 2-(2-bromo-ethyl)-benzo[*de*] isoquinolene-1,3-dione (**3a**), 2-(4-bromo-butyl)-benzo[*de*] isoquinolene-1,3-dione (**3b**) and 4-nitro-1,8-naphthalic anhydride, the starting materials for the synthesis of 2-(2-bromo-ethyl)-6-nitro-benzo[*de*]isoquinolene-1,3-dione (**3c**), were obtained from Sigma–Aldrich, Bangalore, India. 1-Amino-2-ethanol and phosphorous tribromide were from Sigma–Aldrich and were used for synthesis without further purification. *n*-Heptane (Hep), acetonitrile (ACN), tetrahydrofuran (THF), dioxan (DX), *n*-propanol (PrOH), ethanol (EtOH) and methanol (MeOH) were procured from Merck (India). The solvents used in spectral studies, were rigorously purified by standard procedures [24]. The purified solvents were found to be free from impurities and were transparent in the spectral region of interest. Ethanol, ethyl acetate, petroleum ether and chloroform were procured from Merck (India) and used for synthesis. Triply distilled water was used for the preparation of the experimental solutions. Reduced L-glutathione (GSH) was obtained from Sigma, USA and used as received.

2.2. Apparatus and methods

For synthesis all reactions were conducted under anhydrous condition, solvents (ethanol, ethyl acetate, petroleum ether and chloroform) were well dried and reactions were performed using oven-dried glassware. Melting points were determined on a capillary melting point apparatus [SMP3 Apparatus (Bibby, STERILIM, UK)] without correction. NMR spectra were recorded with Brucker AC-300 MHz NMR spectrophotometer on a 300 MHz for proton and 75 MHz for carbon in $CDCl_3$ solution using tetramethylsilane as the internal reference. The coupling constant (*J*) is reported in Hz. Mass spectrum was recorded on JMS600 in EI ionization mass spectrometer. Elementary analyses were recorded on Perkin-Elmer auto analyzer 2400II. Column chromatography was performed using silica gel (60–120 mesh) (Qualigen India).

Shimadzu 1700 model UV–vis spectrophotometer and Spex Fluorolog F-IIA spectrofluorimeter (Spex Inc., NJ, USA) were used for the absorption and fluorescence measurement, respectively. All the experiments were performed with air-equilibrated solutions. For the geometrical optimization, we have used the semiempirical AM1 method and for the determination of ground state energy, dipole moments in the ground and excited state and the transition energies to different excited electronic state, we have used the semiempirical AM1-SCI method supported by Hyperchem 5.01 package from Hypercube Inc., Canada. Utility of the AM1 and AM1-SCI method in getting reliable structural data has already been established [25,26].

The fluorescence quantum yields of the systems were measured using quinine sulfate [27] as the reference compound ($\phi_f = 0.546$ in 1N H_2SO_4). Dilute solution with OD ≈ 0.07 at the excitation wavelength (which typically corresponded to a concentration in the micromolar range) was used for quantum yield measurements. Optically matched solutions of the sample and reference were used. The quantum yields were measured by comparing the areas underneath the fluorescence spectra. All fluorescence spectra were corrected for the instrumental response and each measurement was repeated twice.

2.3. Synthesis

The required derivatives (**3a**–**c**) were synthesized following a two-step procedure as shown in Scheme 1. Compounds **3a** and **3b** were synthesized as reported earlier, which were the intermediate during synthesis of organo selenium compounds. Yield, melting point and related NMR and mass spectral data are therein [28].

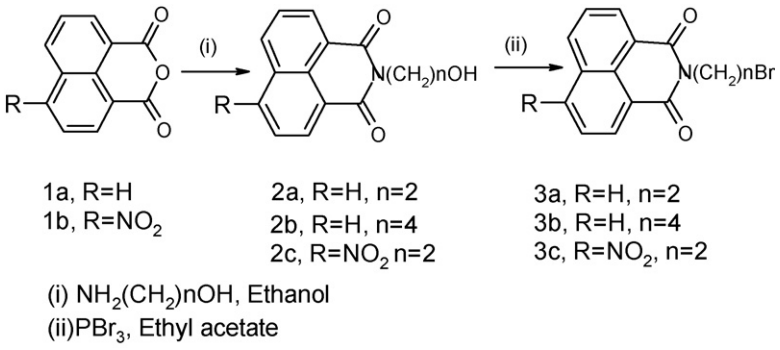

Scheme 1.

4-Nitro-1,8-naphthalic anhydride (**1b**) was first treated with 1-amino-2-ethanol in ethanol to furnish the corresponding 2-(2-hydroxy-ethyl)-6-nitro-benzo[*de*]isoquinolene-1,3-dione (**2c**) which was subsequently treated with phosphorous tribromide to furnish the desired 2-(2-bromo-ethyl)-6-nitro-benzo[*de*]isoquinolene-1,3-dione (**3c**). The exact reaction conditions were as follows.

A mixture of 4-nitro-1,8-naphthalic anhydride (**1b**) (1 g, 0.0041 mol), 1-amino-2-ethanol (0.495 mL, 0.0082 mol) in dry ethanol (25 mL) was heated under reflux for 15 min. The solution was then reduced to half of its initial volume by evaporating ethanol under reduced pressure. The resulting solution was then cooled and the solid separated was filtered and washed with little cold ethanol. The crude solid was crystallized from $CHCl_3$–petroleum ether 60–80 °C to get compound (**2c**) as deep brown colored solid. Yield: 0.97 g (87.0%), mp: 157–160 °C. ^{1}H NMR ($CDCl_3$, TMS = 0.00): 2.05 (1H, s), 3.99 (t, 2H, $=NCH_2$, J = 4.9 Hz), 4.46 (t, 2H, CH_2OH, J = 5.42 Hz), 7.99 (t, 1H, Ar–H, J = 7.50 Hz), 8.40 (d, 1H, Ar–H, J = 7.99 Hz), 8.72 (q, 2H, Ar–H, J = 7.3 Hz), 8.85 (d, 1H, Ar–H, J = 8.75 Hz).

To a stirred suspension of compound **2c** (0.8 g, 2.94 mmol) in ethyl acetate (10 mL) PBr_3 (0.8 mL) was added at room temperature for 20 min. Then the resulting mixture was heated at 70–75 °C with stirring for 1.5 h. The resulting mixture were cooled, poured into ice water and extracted with $CHCl_3$ (100 mL). The extract was washed with saturated $NaHCO_3$ and then with water and dried over $CaCl_2$. Solvent was evaporated under reduced pressure to afford a yellow solid, which was purified by column chromatography over silica gel [petroleum ether (60–80 °C)/$CHCl_3$ (1:1, v/v)] followed by crystallization

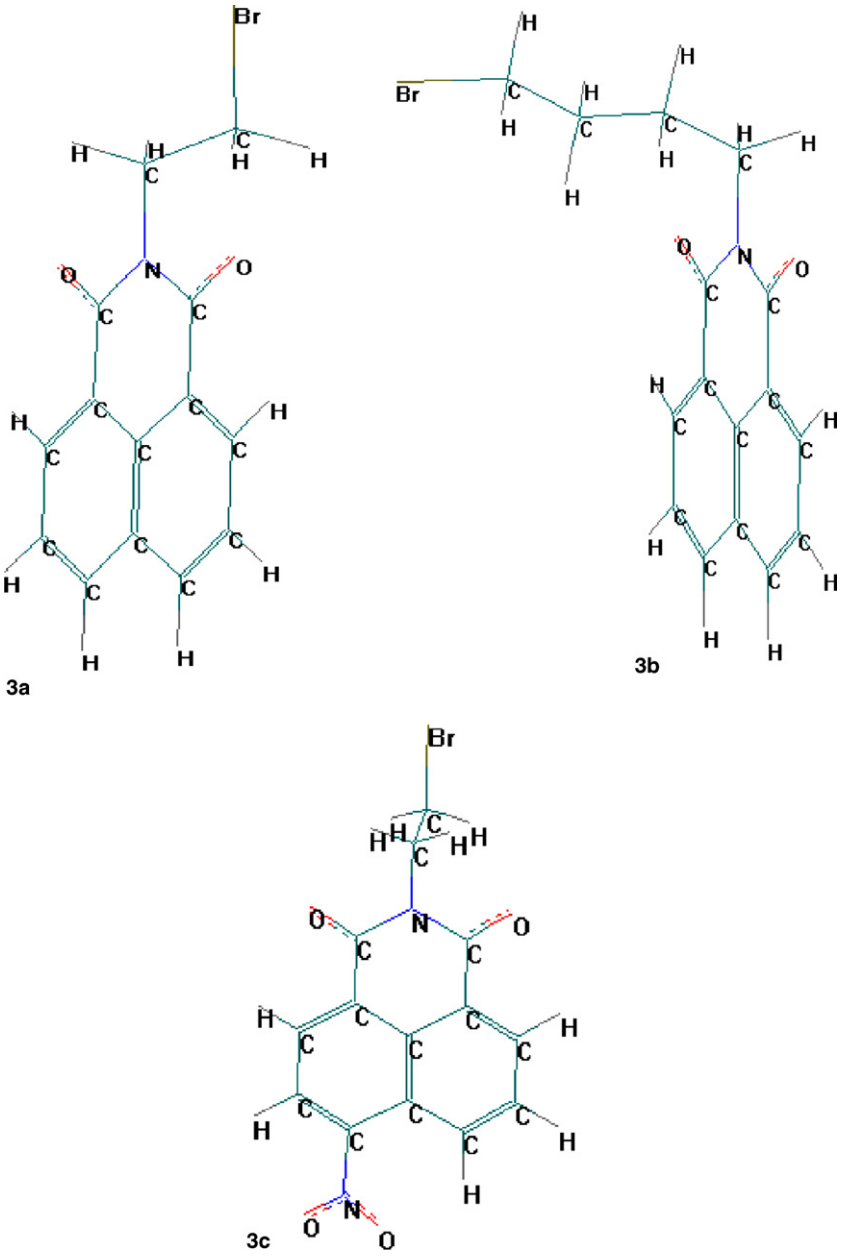

Scheme 2.

from $CHCl_3$ – petroleum ether 60–80 °C to give the desired compound (**3c**). Yield: 0.5 g (51.02%), mp: 190–191 °C ^{1}H-NMR ($CDCl_3$, TMS = 0.00): 3.68 (t, 2H, $=NCH_2$, J = 6.97 Hz), 4.62 (t, 2H, CH_2Br, J = 7 Hz), 8.00 (t, 2H, Ar–H, J = 7.53 Hz), 8.40 (d, 1H, Ar–H, J = 8.01 Hz), 8.73 (q, 2H, Ar–H, J = 7.3 Hz), 8.85 (d, 1H, Ar–H, J = 8.73 Hz). IR (KBr) cm^{-1}: 1708.49 and 1669.22 (amide), 1590.16 (Arom. ring). HRMS (EI+): 349 (M^+, 70%); 348 (M^+, 69); 269 (M^+–Br, 100); 255 (M^+–CH_2Br, 51); 209 (M^+–CH_2Br, –NO_2, 38). ^{13}C (57 MHz, $CDCl_3$): 27.44, 41.45, 122.63, 123.71, 123.86, 126.53, 129.15, 129.64, 129.97, 130.16, 132.76, 149.79, 162.31 and 168.08. Elemental analysis: (found C: 48.02; H: 2.63; N: 7.93. Calculated for $C_{14}H_9BrN_2O_4$; C: 48.16; H: 2.60; N: 8.02).

The optimized geometrical form of the compounds **3a**, **3b** and **3c** are represented in Scheme 2.

3. Results and discussion

3.1. Absorption study

UV–vis absorption spectrum of **3a** in Hep (Fig. 1) has been found to have vibrational splitting and the peak positions are at 315, 325, 329, 341 and 345 nm. In polar protic and polar aprotic solvents absorption maxima shifted to higher wavelength with two distinct peaks at 331 and 344 nm. With variation in polarity of the polar protic and polar aprotic solvents peak position remains unaltered, so polarity of solvent has little influence on the absorption spectra of **3a**. Though the band position of **3a** remains same in polar protic and polar aprotic solvents, molar extinction coefficient in polar protic solvent (EtOH, *n*-PrOH, etc.) is lower compared to the molar extinction coefficient in polar aprotic solvent (ACN, THF, DX, etc.). In ACN and EtOH, absorbance of **3a** is higher in ACN compared to EtOH without any shift in spectral maxima.

Absorption maxima of **3b** remain same to **3a** in Hep and absorption maxima of **3b** shifted to higher wavelength in polar protic and polar aprotic solvent (Fig. 2) identical to **3a**. Absorption maxima of **3b** do not vary with varying polarity of the polar aprotic solvent and hence influence of polarity on **3b** is negligible. In protic polar solvent (EtOH), a new peak appears at 275 nm. The band around 320–340 nm for **3a** has been shifted to 350 nm for **3c**, i.e. there is a red shift in the characteristic absorption band of **3c** compared to **3a**. The absorption maxima shifted to higher wavelength for **3c** due to incorporation of electron withdrawing –NO_2 group at the 4-position. This behavior can be understood taking into consideration of the difference in electron withdrawing ability of the substitute at 4-position and nature of the lowest excited state of the systems. The higher wavelength band for all the compounds may be due to $n \rightarrow \pi^*$ or $\pi \rightarrow \pi^*$ transition.

In photophysical studies of *N*-substituted 1,8-naphthalimide derivatives, it had been reported [22] that the absorption and fluorescence maxima of these molecules had a red shift with increasing value of the dielectric constant of the solvent. This fact takes place in electronic transitions of the type $\pi \rightarrow \pi^*$ with a higher dipole moment in the excited state S_1 than in the ground state S_0 [29]. Dominant electronic transition of 1,8-naphthalimide is the $\pi \rightarrow \pi^*$ transition, as there is a high degree

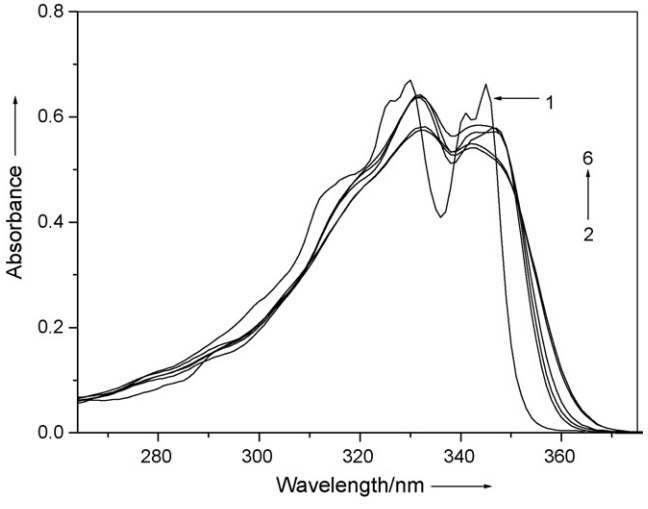

Fig. 1. Absorption spectra of compound **3a** (5.31×10^{-5} mol dm^{-3}) in polar protic and polar aprotic solvents: (1) Hep, (2) *n*-PrOH, (3) EtOH, (4) DX, (5) THF and (6) ACN.

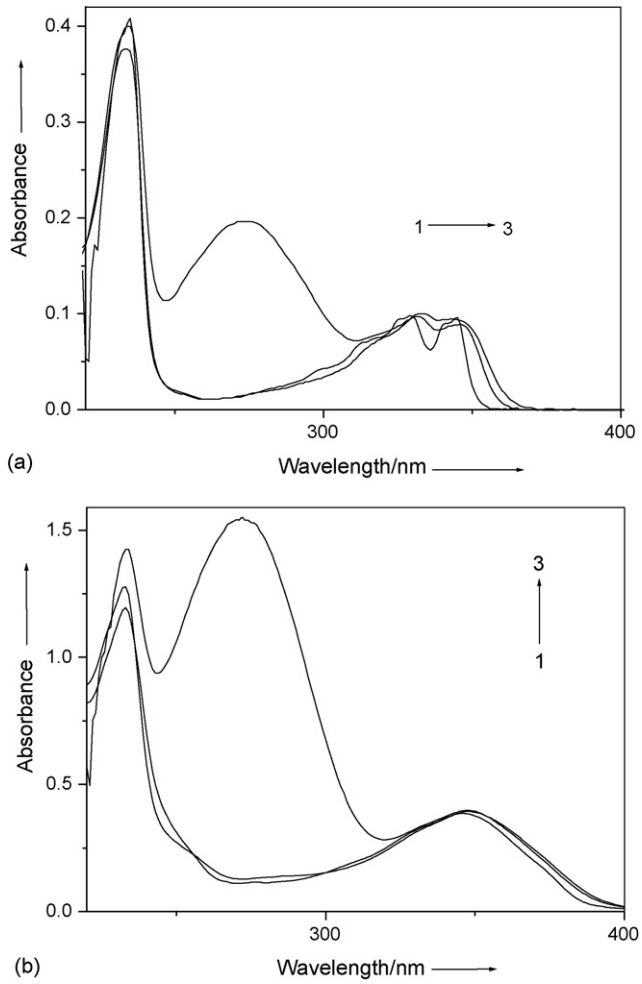

Fig. 2. (a) Absorption spectra of compound **3b** (4.12×10^{-6} mol dm^{-3}) in (1) Hep, (2) ACN and (3) EtOH. (b) Absorption spectra of compound **3c** (1.85×10^{-5} mol dm^{-3}) in (1) Hep, (2) ACN and (3) EtOH.

Table 1
Molar extinction coefficient and quantum yield of compound **3a**, **3b** and **3c** in acetonitrile

Compound	Molar extinction coefficient in ACN ($dm^3\ mol^{-1}\ cm^{-1}$)	Quantum yield in ACN
3a	12022.6 (332), 10989.8 (344)	0.51
3b	23638.4 (332), 21576.1 (345)	0.56
3c	20990.3 (350)	0.01

of coplanarity between the imide and the π system of the naphthalene ring [30]. So the absorption maxima of **3a**, **3b** and **3c** at longer wavelength may be due to $\pi \rightarrow \pi^*$ transition. Molar extinction coefficients (ε) of **3a**, **3b** and **3c** in acetonitrile have been presented in Table 1 and the higher ε value indicates that the transition is $\pi \rightarrow \pi^*$ in nature.

Simultaneously, the newly appeared broad band at the lower wavelength of **3b** and **3c** in polar protic solvents is due to charge transfer to solvent (CTTS). If there is low lying unfilled orbital in the solvent, it is likely to have a strong affinity for electrons. If the solvent accepts the electron from solute molecules, a charge transfer to solvent complex is said to be formed. This charge transfer complexes bridge the gap between the weak vander Waals complexes and the molecule bonded by strong valence force. As the higher energy CTTS band develops in polar protic solvents, so the H-bond between carbonyl group of naphthalimide moiety and protic solvents is responsible for CTTS. For **3a** and **3b** the difference in their structures arises due to the methylene group (spacer) in the side chain, so it is expected that conjugation is less for **3b** and probability of appearance of CTTS band is high for it in their ground state. Expectation coincides with the experimental observation. For **3c** the CTTS band appears in EtOH having higher molar extinction coefficient compared to **3b** due to presence of the nitro group and hence electronic rearrangement occurs which favors CTTS.

3.2. Fluorescence properties

Fluorescence spectra of **3a** in solvents Hep, ACN, DX, THF and EtOH have been given in Fig. 3. On excitation at λ_{max}^{abs} = 345 nm, **3a** displays fairly structured fluorescence spectra having mirror image relationship to the absorption spectra. The fluorescence maxima appears at 366 nm along with two other maxima at higher wavelength 387 and 409 nm in Hep. In polar aprotic solvent ACN, fluorescence maximum has been shifted to 379 nm with shoulders at 363 and 398 nm. With increasing polarity of the aprotic solvents (ACN) fluorescence maxima remains unaltered whereas the fluorescence intensity (peak area) increases. In polar protic solvent (EtOH) the fluorescence maxima shifted to higher wavelength compared to aprotic solvent with a concomitant enhancement of fluorescence intensity. Fluorescence quantum yields of **3a**, **3b** and **3c**, measured in ACN, are collected in Table 1.

In alkane solvent, structured emission of **3a**, showing a mirror image relationship with the corresponding absorption spectrum is ascribed to originate from the locally excited (LE) species with the same ground state geometry. With increasing solvent polarity, the structured fluorescence spectrum gradually looses its resolution. Increase in the solvent polarity induces a remarkable shift in the fluorescence spectra, characteristic of a charge transfer (CT) emission. The observations are similar to those found for other system like coumarines [31], arylaminonaphthalene sulfonates [32], derivatives of bianthryl [33], etc.

Photophysical studies of **3b** in polar aprotic and polar protic solvents reveal an identical spectral feature (Fig. 4). The fluorescence spectrum of **3b** in Hep is identical to that of the fluorescence spectra of **3a** having fluorescence maxima at 366, 387 and 409 nm. In polar aprotic solvent ACN, fluorescence maximum of **3b** has been shifted to 378 nm with shoulders at 361 and 397 nm.

The fluorescence spectrum of **3c** has been depicted in Fig. 5. In Hep, two bands of it has been appeared, one is at 420 nm and the other is at 450 nm. In polar aprotic solvent (ACN), only one band has been observed which is at 450 nm. In polar protic solvent (EtOH), the band is shifted to 460 nm with higher fluorescence intensity compared to ACN. For **3c**, in heptane the structured fluorescence spectra have mirror image relationship to that of the absorption spectra. In polar protic and polar aprotic

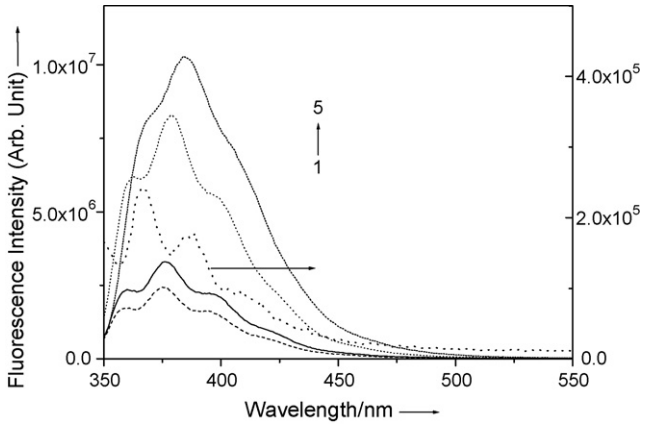

Fig. 3. Fluorescence spectra of compound **3a** (5.31×10^{-5} mol dm^{-3}) in (1) DX, (2) THF, (3) Hep, (4) ACN and (5) EtOH.

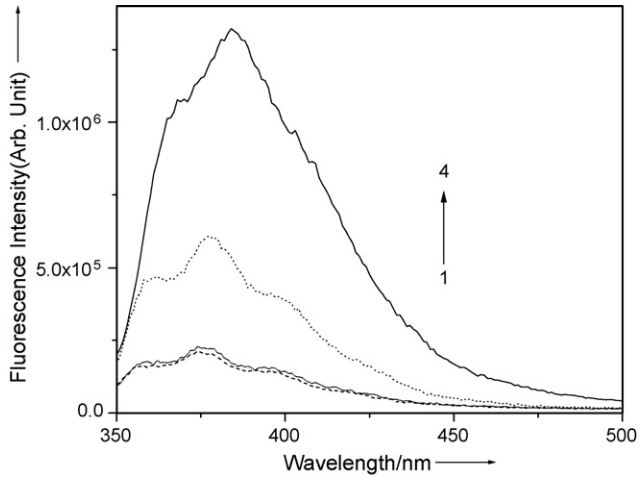

Fig. 4. Fluorescence spectra of compound **3b** (4.12×10^{-6} mol dm^{-3}) in (1) DX, (2) THF, (3) ACN and (4) EtOH.

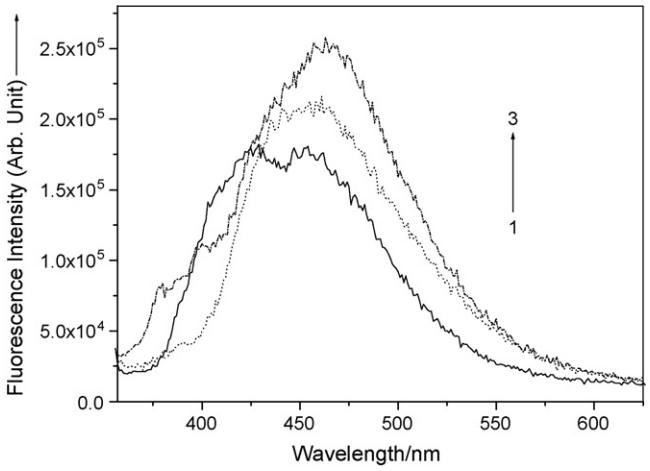

Fig. 5. Fluorescence spectra of compound **3c** (1.85×10^{-5} mol dm^{-3}) in (1) Hep, (2) ACN and (3) EtOH.

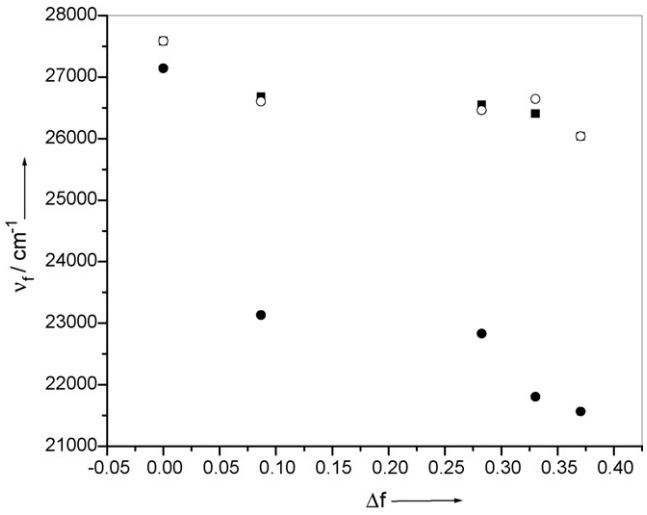

Fig. 6. Dependence of emission maxima (ν_f) as a function of the solvent polarity-polarizability parameter (Δf) for (■) **3a**, (◯) **3b** and (●) **3c**.

solvent the structured fluorescence band has been disappeared at higher wavelength with higher fluorescence intensity. The higher wavelength band in polar solvents has been designated as charge transfer band where the band in alkane solvent is designated as locally excited band. The CT band has also been influenced by hydrogen bonding ability of the solvent. The increase of the stokes shift with increasing solvent polarity suggests that the potential energy surface of the emitting state is considerably different from that of the ground state and a large increase in the excited state dipole moment results a charge transfer character of the fluorescent states.

3.3. Extent of PICT processes from dipole moment

From the fluorescence spectra of **3a**, **3b** and **3c** in different solvents, it has been observed that emission maxima has bathochromic shift with increasing polarity of the solvents. This observation has been interpreted by considering the stabilization of the charge transfer state by the solvent molecules compared to that of the ground state [34]. The extent of increase in the dipole moment of the dye on electronic excitation can be determined from the Lippert–Mataga relation [35], in fairly polar solvents, the relation between the solvent-dependent shift of the emission maxima and the solvent parameter $\Delta f(\varepsilon, n)$ is expressed as follows:

$$\nu_f = \nu_{f0} - \frac{2\,\Delta\mu^2}{4\pi hc\rho^3}\,\Delta f(\varepsilon, n) \quad (1)$$

where $\Delta f(\varepsilon,\ n) = ((\varepsilon - 1)/(2\varepsilon + 1)) - ((n^2 - 1)/(2n^2 + 1))$, ε, n corresponds to the static dielectric constant, the refractive index of the medium, ν_f and ν_{f0} the emission maxima (wavenumbers) in a solvent and in vacuum, $\Delta\mu = (\mu_e - \mu_g)$ the magnitude of the change in the dipole moment on excitation from the ground state to the excited state, h, c, ρ corresponds to Plank's constant (6.6×10^{-34} J s), the velocity of light in vacuum (3.0×10^8 m s^{-1}) and the Onsagar cavity radius. Using the assumption of Lippert, the Onsagar Cavity radius ρ can be derived from the length of the molecule (obtained from AM1 calculation) multiplied by a reduction factor of 0.8 [36].

A plot of the emission maxima ν_f versus the polarity function $\Delta f(\varepsilon, n)$ has been shown in Fig. 6. Least square linear regression analysis gave a good correlation obeying the following relations:

$$\nu_f = 27337.17 - 3196.14\,\Delta f(\varepsilon, n);$$

$$\nu_f = 27286.93 - 2900.65\,\Delta f(\varepsilon, n);$$

$$\nu_f = 25908.07 - 12213.36\,\Delta f(\varepsilon, n)$$

for compounds **3a**, **3b** and **3c**, respectively.

According to Eq. (1) it approximately corresponded to the difference in dipole moment of 1.87 D, 1.83 D and 4.22 D for **3a**, **3b** and **3c**, respectively, for the charge transfer state relative to the ground state. The difference in dipole moments for locally excited band was 0.25 D, 0.22 D and 1.11 D, respectively, calculated by AM1 and AM1-SCI calculation. So, this was due to intramolecular charge transfer from bromo group to the 1,8-naphthalimide moiety. The bromo group has less efficiency of charge transfer and hence in ground state charge transfer process does not appear. In absorption spectra of **3a**, **3b** and **3c** no intramolecular charge transfer band appears, so the appeared band in the excited state is photoinduced intramolecular charge transfer (PICT) band. In polar protic solvents PICT process is favoured over the polar aprotic solvents and hence the carbonyl group of naphthalimide moiety has an assisting influence on PICT process which has been verified in the latter section.

The only difference between **3a** and **3b** arises due to different number of carbon atoms in the spacer, i.e. the distance between receptor and fluorophore. From theoretical calculation it is evident that the difference of dipole moment of locally excited states and charge transfer state between **3a** and **3b** is low. Whereas a high difference in dipole moment arises between **3a** and **3c** and this effect has been rationalized in terms of introduction of electron withdrawing nitro group into **3a** to form **3c**.

3.4. Excited state interaction of *3a*, *3b* and *3c* with reduced L-glutathione

The aqueous solution of **3a**, **3b** and **3c** exhibit higher fluorescence intensity and the fluorescence maxima shifted to higher wavelength from **3a** to **3c**. On gradual addition of GSH in the aqueous solution of **3a**, fluorescence intensity decreases at $\lambda^{fl}_{max} = 450$ nm with concomitant increase in emission intensity at $\lambda^{fl}_{max} = 398$ nm (Fig. 7a). An isoemmisive point has been observed at 420 nm. In case of compound **3b**, emission maximum remains unaltered in presence and absence of GSH but fluorescence intensity of **3b** decreases with increasing concentration of GSH (Fig. 7b). On gradual addition of GSH in the aqueous solution of **3c**, emission maxima and emission intensity remains unaltered. Addition of GSH in aqueous solution makes a redistribution of the water cage formed by surrounding water molecules and GSH formed H-bond to the compounds. In **3c** GSH has no influence to alter the PICT process whereas for **3a** it has little influence. But for **3b** the PICT process has been drastically decreased due to addition of GSH. H-bonding solvent can enhance the PICT process of N-substituted 1,8-naphthalimide derivatives. The presence of nitro group in **3c** can form a compact cage of water surrounding **3c** and hence GSH cannot form hydrogen bond with **3c**.

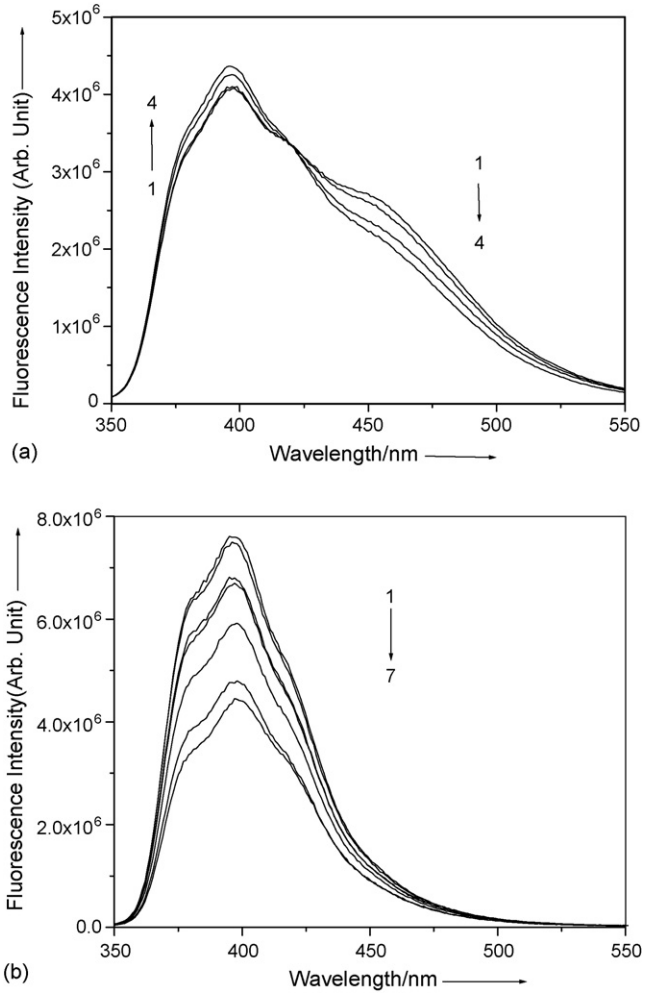

Fig. 7. (a) Fluorescence spectra of compound **3a** in aqueous solution of GSH where [GSH]: (1) 0 mM, (2) 0.1 mM, (3) 0.4 mM and (4) 0.8 mM. (b) Fluorescence spectra of compound **3b** in aqueous solution of GSH where [GSH]: (1) 0 mM, (2) 0.05 mM, (3) 0.2 mM, (4) 0.25 mM, (5) 0.4 mM, (6) 0.6 mM and (7) 0.08 mM.

4. Conclusions

In the absorption spectra of **3a**, **3b** and **3c**, one band arises due to $\pi \rightarrow \pi^*$ transition at the longer wavelength and for **3b** and **3c** a new band arises at shorter wavelength due to charge transfer to solvent. The excited state fluorescence spectra composed of two types of bands—one due to locally excited band appeared in nonpolar solvents and in polar solvent photoinduced charge transfer band arises at longer wavelength. Protic solvent assists the photo induced charge transfer process of the compounds.

Acknowledgments

Financial assistance from DRDO (No. ERIP/ER/0103338/M/01), India and CSIR [No. 1 (1728)/02/EMR-II], India, are gratefully acknowledged. One of the author (S.C.) thanks Jadavpur University for laboratory facilities. One of the author (S.U.H.) gratefully acknowledges CSIR for SRF.

References

[1] A. Da Settimo, G. Primofiore, P.L. Ferrarini, M. Ferretti, P.L. Barili, N. Tellini, P. Bianchini, Eur. J. Med. Chem. 24 (1989) 263.
[2] L. Saito, Pure Appl. Chem. 64 (1992) 1305.
[3] M.R. Kirshenbaum, S.-F. Chen, C.H. Behrens, L.M. Papp, M.M. Stafford, J.-H. Sun, D.L. Behrens, J.R. Fredericks, S.T. Polkus, P. Sipple, A.D. Patten, D. Dexter, S.P. Seitz, J.L. Gross, Cancer Res. 54 (1994) 2199.
[4] A. Dorlars, C.-W. Schellhammer, J. Schroeder, Angew. Chem. Int. Ed. Engl. 14 (1975) 665.
[5] W.W. Stewart, Nature 292 (1981) 17.
[6] M.F. Brana, J.M. Castellano, C.M. Roldan, A. Santos, D. Vazquez, A. Jimenez, Cancer Chemother. Pharmacol. 4 (1980) 61.
[7] M.F. Brana, J.M. Castellano, A.M. Sanz, C.M. Roldan, Eur. J. Med. Chem. 16 (1981) 207.
[8] D. Rideout, R. Schinazi, C.D. Pauza, K. Lovelace, L.C. Chiang, T. Calogeropoulou, M. McCarthy, J.H. Elder, J. Cell. Biochem. 51 (1993) 446.
[9] T.C. Chanh, D.E. Lewis, J.S. Allan, B.F. Sogandares, M.M. Judy, R.E. Utecht, J.L. Matthews, AIDS Res. Hum. Retroviruses 9 (1993) 891.
[10] T.C. Chanh, B.J. Archer, R.E. Utecht, D.E. Lewis, M.M. Judy, J.L. Matthews, Biomed. Chem. Lett. 3 (1993) 555.
[11] T.C. Chanh, D.E. Lewis, M.M. Judy, B.F. Sogandares, G.R. Michalek, R.E. Utecht, H. Skiles, J.L. Matthews, Antiviral Res. 25 (1994) 133.
[12] D. Rideout, R. Schinazi, C.D. Pauza, K. Lovelace, L.C. Chiang, T. Calogeropoulou, M. McCarthy, J.H. Elder, J. Cell. Biochem. 51 (1993) 446.
[13] A. Demeter, T. Berces, L. Biczok, V. Wintgens, P. Valat, J. Kossanyi, J. Phys. Chem. 100 (1996) 2001.
[14] A. Demeter, L. Biczok, T. Berces, V. Wintgens, P. Valat, J. Kossanyi, J. Phys. Chem. 97 (1993) 3217.
[15] P. Valat, V. Wintgens, J. Kossanyi, L. Biczok, A. Demeter, T. Berces, J. Am. Chem. Soc. 114 (1992) 946.
[16] K.-A. Mitchell, R.G. Brown, Y. Dongwu, S. Chang, R.E. Utecht, D.E. Lewis, J. Photochem. Photobiol. A 115 (1998) 157.
[17] M.S. Alexiou, V. Tychopoulos, S. Ghorbanian, J.H.P. Tyman, R.G. Brown, P.I. Brittain, J. Chem. Soc. Perkin Trans. 2 (1990) 83.
[18] D. Yuan, R.G. Brown, J. Phys. Chem. A 101 (1997) 3461.

[19] A. Samanta, B. Ramachandram, G. Saroja, J. Photochem. Photobiol. A 101 (1996) 29.
[20] B. Ramachandram, N.B. Sankaran, R. Karmakar, S. Saha, A. Samanta, Tetrahedron 56 (2000) 7041.
[21] S. Saha, A. Samanta, J. Phys. Chem. A 106 (2002) 4763.
[22] E. Martin, R. Weigand, A. Pardo, J. Lumin. 68 (1996) 157.
[23] G. Mugesh, H.B. Singh, Chem. Soc. Rev. 29 (2000) 347.
[24] I.L. Finar, Organic Chemistry I, sixth ed., ELBS, 1973, p. 890.
[25] T.A. Engeland, T. Bultmann, N.P. Earnsting, M.A. Rodriguez, W. Thiel, Chem. Phys. 163 (1992) 43.
[26] J. Catalan, F. Fabero, M.S. Guijarro, R.M. Claramunt, M.D. Santa Maria, M.C. Foces-Foces, F.H. Cano, J. Elguero, R. Sastre, J. Am. Chem. Soc. 112 (1990) 747.
[27] J.N. Demas, G.A. Crosby, J. Phys. Chem. 75 (1971) 991.
[28] S.U. Hossain, S. Sengupta, S. Bhattacharya, Bioorg. Med. Chem. 13 (2005) 5750.
[29] N.J. Turro, Modern Molecular Photochemistry, Benjamin/Cummings, Menlo Park, CA, 1978.
[30] T.C. Barros, G.R. Molinari, P. Berci Filho, V.G. Toscano, M.J. Politi, J. Photochem. Photobiol. A 76 (1995) 55.
[31] F. Cichos, A. Willert, U. Rempel, C.V. Borczyskowski, J. Phys. Chem. A 101 (1997) 8179.
[32] E.M. Kosower, Acc. Chem. Res. 15 (1982) 259.
[33] J.J. Piet, W. Schuddeboom, B.R. Wegewijs, F.C. Grozema, J.M. Warman, J. Am. Chem. Soc. 123 (2001) 5337.
[34] J. Hicks, M. Vandersall, Z. Babaogic, K.B. Eisenthal, Chem. Phys. Lett. 116 (1985) 18.
[35] P.R. Bangal, S. Panja, S. Chakravorti, J. Phys. Chem. A 139 (2001) 5.
[36] S.A. Lyazidi, M. Dkaki, N. Bitit, D. Meziane, C.C. Dubroca, Ph. Cazeau, Spectrochim. Acta (Part A) 55 (1999) 89.